Articles

Dynamics of DNA Condensation†

Dietmar Porschke

ABSTRACT: The condensation of DNA induced by spermine and spermidine is investigated by equilibrium titrations and stopped-flow and field-jump experiments using scattered light detection. The spermine concentration required for the cooperative condensation process is measured at different DNA concentrations; these data are used to evaluate both the condensation threshold degree of spermine binding and the binding constant of spermine according to an excluded-site model. Stopped-flow measurements of the spermine-induced condensation demonstrate the existence of two processes: (1) A "fast" reaction is observed in the millisecond time range, when the reactant concentrations are around 1 μM; it is associated with a characteristic induction period and is assigned to the *intra*molecular condensation reaction. (2) A slow reaction with time constants of, e.g., 100 s strongly dependent upon both spermine and DNA concentrations is assigned to an *inter*molecular DNA association. The unusual time course of the *intra*molecular condensation reaction with the induction period provides evidence for a "threshold kinetics". During the induction period, spermine molecules are bound to DNA, but the degree of binding remains below the threshold value. As soon as the degree of ligand binding arrives at the threshold, the DNA is condensed in a relatively fast reaction. Model calculations of the spermine binding kinetics according to an excluded-site model demonstrate that the spermine molecules bound to DNA are mobile along the double helix. A comparison of the experimental data with the results of Monte Carlo simulations suggests a rate constant of $\sim 200\ s^{-1}$ for spermine movement by one nucleotide residue. The dissociation rate of DNA–spermine condensates obtained from stopped-flow measurements is shown to be determined by spermine dissociation, even though the decondensation is faster by a factor of about 10 than the dissociation of individual spermine molecules. The acceleration is due to a statistical factor resulting from the fact that the dissociation of some spermine molecules out of a high number of bound molecules is sufficient to induce decondensation. Interpretation of the experimental data in terms of a simple model suggests that the decondensation proceeds in units of about 60 base pairs. The condensation dynamics in the limit of high ligand concentrations, studied by field-jump experiments, are reflected by a spectrum of time constants ranging from 25 μs to 2 ms. The high rate of DNA condensation indicates a remarkable flexibility of the double helix with very fast bending motions.

DNA is often found in very compact structures. The tight packing of DNA in, e.g., chromatin (Sperling & Klug, 1977) or phage heads (Earnshaw & Harrison, 1977; Earnshaw et al., 1978) has been analyzed mainly with respect to the structure of the "condensed" DNA. Relatively little attention has been given to the dynamics of DNA packing, although the dynamics of this process will also be essential for the biological function. Since the DNA packing is expected to be a rather complex process, it should be studied first in a relatively simple system. An appropriate model system of direct biological relevant is the spermine-induced DNA condensation. It has been shown by Gosule & Schellman (1976, 1978) that the condensation of DNA induced by spermine or spermidine at low concentrations is an intramolecular process. Chattoray et al. (1978) demonstrated that the condensation product is a well-ordered toroidal structure. Wilson & Bloomfield (1979) found that DNA is condensed when a critical fraction of the DNA phosphate charges are neutralized by counterions. As shown by Widom & Baldwin (1980), spermine or spermidine can be replaced by ions like Co^{3+}-$(NH_3)_6$. These observations indicate that the ligands are mainly required to reduce the charge density of DNA to a sufficiently low level before the DNA is condensed. According to these results, it may be expected that the coupling between ligand binding and the DNA conformational change is essential for the dynamics as well. The main goal of the present investigation is the characterization of the intramolecular condensation reaction starting from a wormlike coil of DNA and resulting in a well-ordered torus. To avoid intermolecular DNA condensation, the measurements had to be conducted at very low concentrations. This requirement together with the necessity to mix DNA and spermine quickly without shearing of DNA caused some technical problems. The results obtained provide new information on the dynamics of DNA and also on the dynamics of ligand binding. It is expected that the proposed mechanism is relevant also for other cases of DNA packing.

Materials and Methods

λ-DNA was obtained from Boehringer Mannheim and T4 DNA from Miles Laboratories, Elkhart, IN. T7 DNA was isolated by repeated phenol extractions from phages that were kindly provided by Dr. Ch. Biebricher, Gottingen, FRG, and Prof. M. Schweiger, Innsbruck, Austria. All DNA samples were dialyzed extensively against 1 mM NaCl, 50 μM ethylenediaminetetraacetic acid (EDTA), and 1 mM sodium cacodylate, pH 6.4, used as a standard buffer for most measurements. For the titration experiments at different ionic strengths, the salt concentration was adjusted by addition of NaCl. Spermine·4HCl and spermidine·3HCl were obtained from Serva, Heidelberg, FRG.

Scattered light intensities were measured as a function of spermine or spermidine concentration by an Aminco SPF 500 fluorometer. Usually the scattered light was measured at 290 nm. Stopped-flow experiments were performed with an in-

† From the Max-Planck-Institut für biophysikalische Chemie, 34 Gottingen, FRG. *Received January 31, 1984.*

0006-2960/84/0423-4821$01.50/0

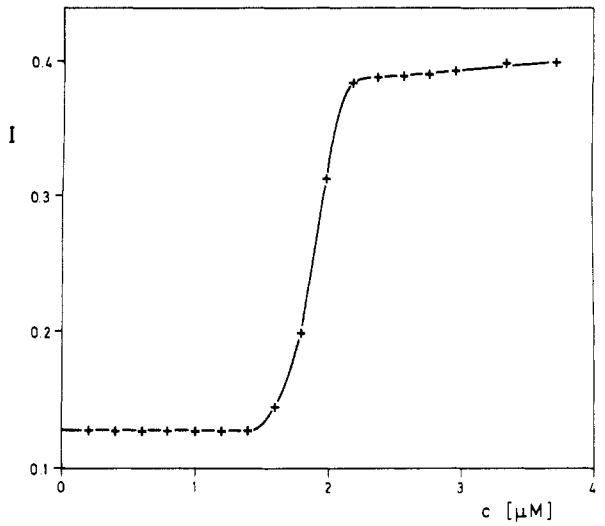

FIGURE 1: Scattered light intensity I (relative units) of 8 μM λ-DNA as a function of the spermine concentration c (λ = 290 nm; 4 mM NaCl, 4 mM sodium cacodylate, pH 6.4, and 0.2 mM EDTA).

strument constructed at this institute. The solutions did not have any contact with metal parts; the temperature was controlled by a closed circulation system. Changes in the scattered light intensity were recorded on a Biomation 1010 transient recorder and sent to the computer center of the Gesellschaft fur wissenschaftliche Datenverarbeitüng mbH, Göttingen, FRG. Due to the relatively high noise of single stopped-flow curves at DNA concentrations in the micromolar range, the signal to noise ratio was improved by averaging of usually 20 stopped-flow experiments. Field-jump experiments were performed as described (Porschke et al., 1984). The standard temperature in all experiments was 20 °C.

Results

Equilibrium Titrations. As may be expected for this type of ligand-induced intramolecular process, the degree of ligand binding to the DNA must exceed a limit value, θ_δ, to induce condensation. Experimental evidence for this effect has been presented for various types of ions like spermine, spermidine, putrescine, Mg^{2+}, and $Co^{3+}(NH_3)_6$ (Wilson & Bloomfield, 1979). Since the DNA condensation is a cooperative process, the overall ligand concentration required for the transition can be determined with high accuracy. Measurements of the total ligand concentration corresponding to θ_δ at different DNA concentrations should provide information about the binding equilibrium. We have used this approach to determine equilibrium constants for the binding of spermine to DNA according to an excluded-site model. The condensation of DNA was usually characterized by simple scattered-light titrations performed with a conventional spectrofluorometer (cf. Figure 1). In some cases, the transition was also characterized by field-jump experiments (see below).

From the titration experiments, we obtain a series of total ligand concentrations, c_δ, required to induce condensation at given DNA concentrations, c_p (in units of nucleotide residues). A set of these values may be used to compute both the constant K for the association of spermine to DNA and the limit degree of binding θ_δ according to an excluded-site binding model (McGhee & von Hippel, 1974). θ_δ is defined in units of nucleotide residues covered by spermine at the midpoint of the transition relative to the total number of nucleotide residues. The number of nucleotide residues covered by one spermine molecule is assumed to be four, corresponding to the number of positive charges associated with spermine. A least-squares

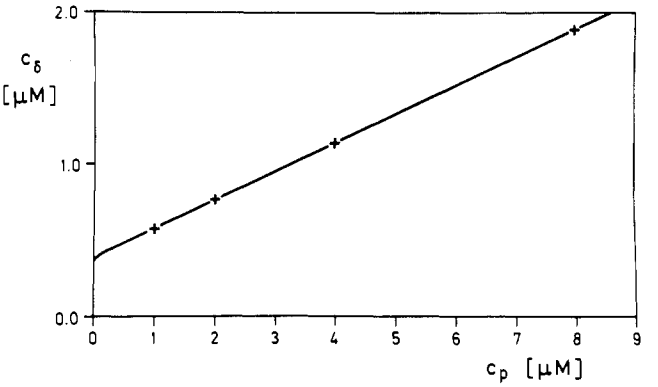

FIGURE 2: Spermine concentration c_δ at the midpoint of the condensation transition as a function of the DNA concentration c_p (in monomer units; 4 mM NaCl, 4 mM sodium cacodylate, pH 6.4, and 0.2 mM EDTA). The line represents a least-squares fit according to an excluded-site model (cf. text); $K = 9.8 \times 10^6$ M^{-1}; $\theta_\delta = 0.746$.

Table I: Threshold Degree of Spermine Binding (θ_δ) and Association Constant (K) of Spermine to DNA as a Function of the Ionic Strength (I_μ) according to an Excluded-Site Model

I_μ (mM)	θ_δ	K (M^{-1})
1.75	0.86	5.9×10^8
3.5	0.83	7.3×10^7
5.25	0.805	3.8×10^7
7.0	0.75	1.0×10^7
17	0.7	1.4×10^6

fit of data measured in an appropriate concentration range provides clear error minima for K and θ_δ (cf. Figure 2). Measurements at various salt concentrations, I_μ, reveal the expected decrease of K with increasing I_μ (cf. Table I). An analysis of this salt dependence according to polyelectrolyte theory suggests that the number of charges compensated upon complex formation is ~2.7. This is rather close to the value 3.3 obtained previously from dialysis experiments in the range of salt concentrations around 0.1 M (Braunlin et al., 1982).

Stopped-Flow Measurements of the Condensation Reaction. Simple mixing of DNA with spermine in a cuvette and observation of the reaction by scattered-light measurements demonstrate that spermine induces two different types of condensation reactions. At 1 μM DNA, the change of scattered light induced by addition of, e.g., 1 μM spermine is almost complete during the few seconds required for mixing. At higher concentrations of DNA and, in particular, of spermine, a relatively large part of the scattered-light change is observed in the time range >5 s. The contribution of the slow reaction at a given spermine concentration is increased by an increase of the DNA concentration, indicating that the slow reaction is mainly due to intermolecular association of DNA. Thus, the intramolecular process is associated with the fast change of scattered light that cannot be resolved by a simple mixing experiment. The characterization of the fast intramolecular condensation requires a stopped-flow technique with a sufficiently high sensitivity to measure scattered-light changes at very low concentrations.

Initial attempts to follow the reaction with a conventional stopped-flow apparatus were not successful. Analysis of DNA samples subjected to stopped-flow experiments demonstrated that the long DNA molecules were strongly sheared to short fragments. This was reflected in the kinetic curves by rather small contributions from the expected intramolecular condensation together with relatively large scattered-light changes in the time range >1 s due to intermolecular association resulting from the increased molar concentration of strands (at constant concentration of monomer residues).

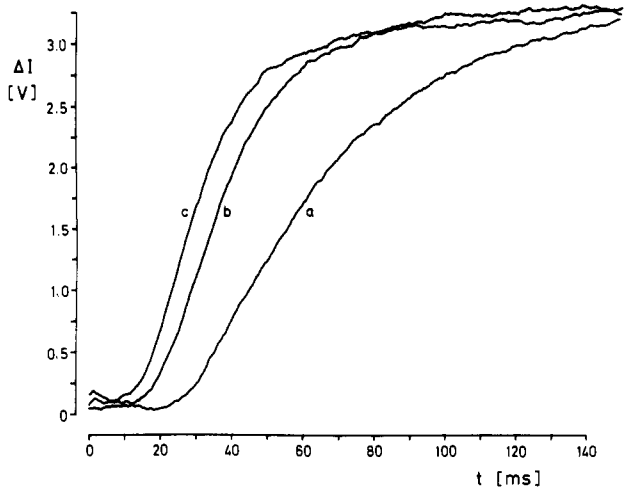

FIGURE 3: Change of the scattered light intensity ΔI as a function of the time t after mixing of 1 μM T4 DNA with (a) 0.7, (b) 1.0, and (c) 1.5 μM spermine (standard buffer, 20 °C).

Since the shearing of DNA is caused by the high flow rate associated with turbulence in stopped-flow experiments, the flow rate had to be reduced at the expense of time resolution. Various modifications of the stopped-flow apparatus were tested to achieve a reliable low flow rate. Finally, the introduction of a narrow channel behind the observation chamber proved to be most useful. By variation of the channel diameter, it was possible to adjust any desired flow rate with high reproducibility.

When the flow rate was decreased, the contribution of the fast process increased, whereas the amplitude of the slow process decreased. At a flow rate around 3 μL/ms, most of the amplitude was observed in a time range >5 s as expected from simple mixing experiments without great shearing gradients. Analytical ultracentrifugation of a λ-DNA sample subjected to a stopped-flow experiment at this low flow rate demonstrated that the molecular weight remained unaffected.

As shown in Figure 3, the spermine-induced DNA condensation is a relatively fast reaction, which can be resolved by stopped-flow experiments at reduced flow rates only for very low reactant concentrations. When the spermine concentration is higher than 2 μM (at a DNA concentration of 1 μM), part of the reaction shown in Figure 3 cannot be observed anymore due to the limited time resolution. The condensation reaction reflected by an increase of scattered light requires a period of induction. The induction time decreases with increasing spermine concentration. These data indicate that the condensation is a two-step reaction and suggest the following simple interpretation. In the first step, the spermine ligands bind to the DNA; when the degree of binding arrives at a limit value, the DNA is condensed in a subsequent reaction step. The sequence of reactions may be described by the following equations, where S denotes spermine molecules:

$$\mathrm{DNA_{free}} + \mathrm{S} \underset{k_s^-}{\overset{k_s^+}{\rightleftharpoons}} \mathrm{DNA_{free}{\cdot}S_1} \quad (1)$$

$$\mathrm{DNA_{free}{\cdot}S_n} + \mathrm{S} \underset{k_s^-}{\overset{k_s^+}{\rightleftharpoons}} \mathrm{DNA_{free}{\cdot}S_{n+1}} \quad (2)$$

$$\mathrm{DNA_{free}{\cdot}S_m} \underset{k_c^-}{\overset{k_c^+}{\rightleftharpoons}} \mathrm{DNA_{condensed}{\cdot}S_m} \quad (3)$$

The DNA lattice is filled with spermine molecules in many reaction steps, which are not seen directly by the measurements of light scattering. When the number of bound spermine molecules arrives at a limit m, the DNA is converted from the free to the condensed form, which is detected by a strong increase of light scattering.

At high spermine concentrations, the change of light scattering is too fast to be detected by the stopped "slow" flow apparatus. This result indicates that the condensation reaction described by eq 3 is a fast process. Furthermore, it may be concluded that the rate of DNA condensation observed at low spermine concentrations is determined by the many steps of spermine association described by eq 1 and 2. The kinetics of condensation were found to be very similar for the different DNA samples from λ, T4, and T7 phages.

Intermolecular Association. At low concentrations of spermine ($c \leq 2$ μM), the change of scattered light appears to be almost complete within 1 s. When the spermine concentration is increased to 5 or 10 μM, an increasing amplitude in the time range around 100 s is observed. It is possible to represent this process by a single exponential. The time constant is dependent upon both the DNA and the spermine concentrations. When spermine is in excess at a constant level, the reciprocal relaxation time increases linearly with the nucleotide concentration. This result demonstrates that the slow process reflects an association reaction of DNA strands. In the absence of detailed information on the type of association, it is assumed that the DNA molecules associate according to an isodesmic reaction model (without limit in the number of DNA molecules associating with each other). The reciprocal relaxation time according to this model is given by

$$1/\tau = 2k_a^+ c_s + k_a^- \quad (4)$$

where k_a^+ and k_a^- are the rate constants of association and dissociation, respectively, and c_s is the concentration of free sites (Porschke & Eggers, 1972). A least-squares fit of data obtained for λ DNA in the presence of 10 μM spermine provided the following rate constants: $k_a^+ = 8.9 \times 10^3$ $\mathrm{M^{-1}}$ (nucleotides) $\mathrm{s^{-1}}$; $k_a^- = 1.13 \times 10^{-3}$ $\mathrm{s^{-1}}$. When the association rate constant is given in units of polymer concentration, the resulting value of 8.2×10^8 $\mathrm{M^{-1}}$ (polymer) $\mathrm{s^{-1}}$ is in an order of magnitude close to the limit of diffusion control expected for a reaction between condensed DNA strands of $\sim 32 \times 10^6$ daltons.

Decondensation. The stopped-flow technique may also be used to characterize the dissociation of condensed DNA. The dissociation reaction was induced by mixing of condensed DNA with a sufficient quantity of free DNA. Due to binding of spermine to the free DNA, the concentration of free spermine is reduced below the threshold value. Since the degree of spermine binding to the added DNA remains below the limit required for condensation, the trapping of spermine by added DNA does not affect the measured intensity of scattered light. The dissociation of condensed DNA observed in these experiments cannot be described by a single exponential. The change of scattered light exhibits a small, but clearly visible, induction period (Figure 4). The main part of the scattered-light change is associated with a time constant of about 0.6 s. Measurements at different concentrations of added free DNA did not reveal any concentration dependence within the limits of accuracy. These experiments indicate that the decrease of the free spermine concentration by the added DNA is fast enough and does not influence the dissociation curves.

From the data described above, it is not possible yet to decide whether the rate of decondensation is determined by the dissociation of spermine or by the unfolding of the DNA itself. This question may be answered by measurements with DNA condensed by spermidine. According to all information available, the structure of DNA condensed by spermine is very

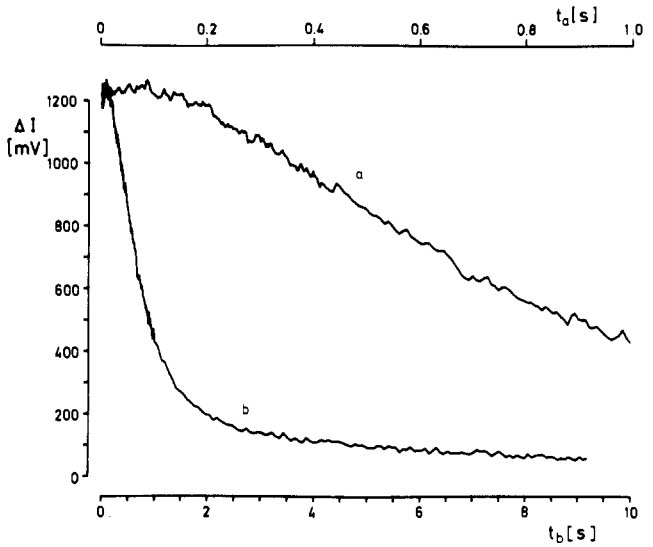

FIGURE 4: Change of the scattered light intensity ΔI as a function of the time t after mixing of 8 μM λ-DNA + 2.6 μM spermine with 8 μM DNA (from calf thymus, sonicated) represented at two different time scales, a and b.

similar to that condensed by spermidine. Thus, the dissociation rates of these DNA condensates should be very similar, if the rate is mainly determined by DNA unfolding. However, stopped-flow measurements demonstrate that the dissociation of spermidine–DNA condensates is much faster than that observed for spermine–DNA condensates. The time constants found in the range around 5 ms in the case of spermidine demonstrate that the decondensation rate—at least for the DNA condensed by spermine—is determined by the dissociation of the ligand. The increase of the decondensed rate in the case of spermidine by a factor of about 100 is consistent with the fact that the binding constant of spermidine is lower than that of spermine by about the corresponding order of magnitude.

Monte Carlo Simulations. As mentioned above, the condensation of DNA must be described by two different types of reaction. In the first step, spermine (or a corresponding ligand) binds to DNA. When the charge density of the DNA is reduced by association of a sufficient number of spermine molecules, the DNA is contracted to the condensed state. It is known from the equilibrium titrations that the degree of spermine binding (θ) must exceed a limit value to induce the condensation reaction. In the standard buffer used for the kinetic experiments, this value was found to be $\theta_\delta = 0.86$ (cf. Equilibrium Titrations). Since spermine molecules with their four positive charges will compensate the corresponding number of phosphate charges, the kinetics of spermine binding will be strongly influenced by excluded-site effects (Epstein, 1979). These effects are illustrated in Figure 5. Obviously spermine will bind to the DNA at random positions. Since spermine molecules cover four nucleotides residues, the random association of ligand molecules will lead to a distribution which excludes further association even though the DNA lattice is not yet completely occupied. However, more ligands may be bound to the DNA when the distribution of ligands along the polymer chain is rearranged. This may be accomplished by dissociation of ligands and subsequent binding at different sites. Since dissociation is usually a slow reaction, redistribution of ligands according to this mechanism is a relatively slow process. However, the redistribution may be accelerated by sliding and/or hopping of ligands along the polymer. Due to the complexity of reactions, it is difficult to describe the "excluded site" kinetics by analytical methods. Thus, a quantitative

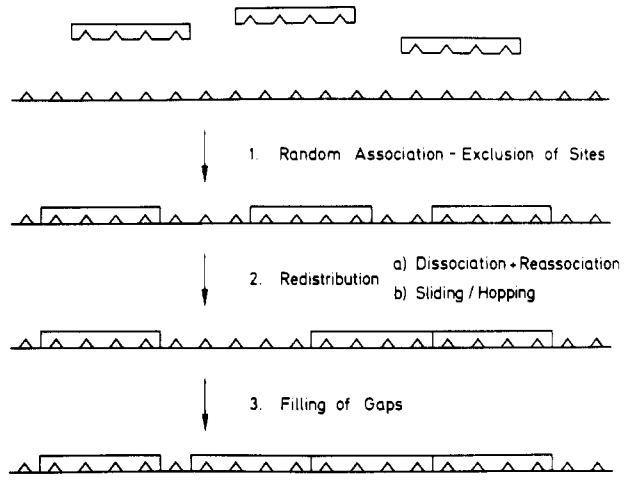

FIGURE 5: Dynamics of excluded-site binding for a ligand that covers four residues (cf. text).

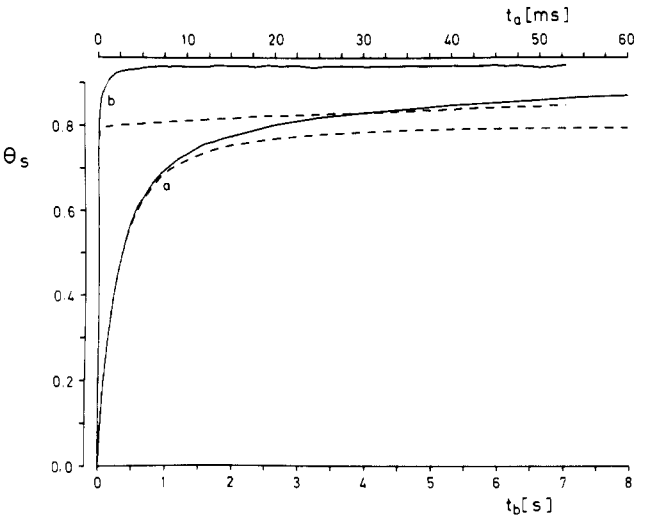

FIGURE 6: Degree of spermine binding θ_s as a function of the time t according to a Monte Carlo simulation: $k_s^+ = 1 \times 10^8$ M^{-1} s^{-1}, $k_s^- = 0.17$ s^{-1}, length of the lattice 200 residues, residue concentration 1 μM, spermine concentration 1 μM, mobility $k_m = 0$ (dashed line), and $k_m = 200$ residues per second (solid line). The curves represent the average of 100 simulations and are plotted in two different time scales, a and b.

analysis of excluded-site processes—at least at high degrees of binding—requires numerical procedures.

A Monte Carlo simulation (Epstein, 1979) of spermine binding to DNA using an estimated association rate constant of 10^8 M^{-1} (nucleotides) s^{-1} shows that the degree of binding may quickly approach a value of about $\theta = 0.8$. However, the further increase toward the equilibrium value of θ is very slow due to the low rate of spermine dissociation. According to the simulation shown in Figure 6, it takes more than 5 s to arrive at a value $\theta_\delta = 0.86$ required for DNA condensation. This is a very long time compared to the time constants observed in the stopped-flow experiments. However, the approach to the limit value of θ may be strongly accelerated by assuming some mobility of spermine molecules along the double helix. When the rate of spermine motion is $k_m = 200$ s^{-1}, corresponding to a time constant for a shift by one "lattice" residue of 5 ms, the degree of binding is 0.86 already within approximately 15 ms (at the same concentrations and k_s^+ and k_s^- values as used above). Thus, it should be possible to evaluate the mobility of spermine ligands on DNA helices by comparison of experimental and simulated reaction progress curves. For this purpose, spermine binding has been simulated for sets of 150 single, separate lattices, providing a distribution

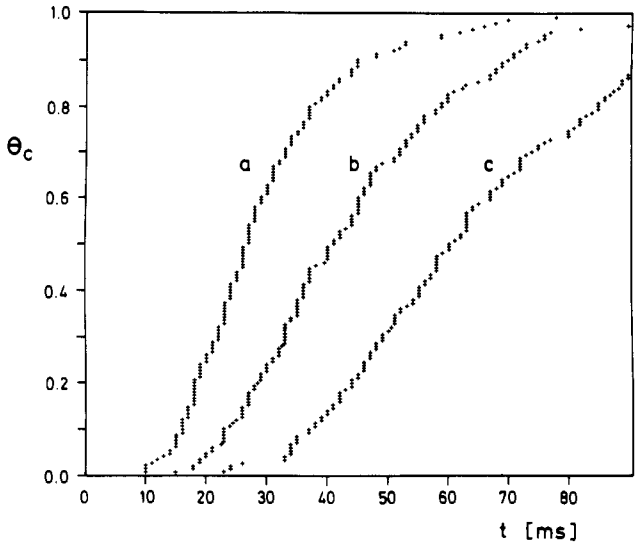

FIGURE 7: Degree of DNA condensation θ_c as a function of the time t according to a Monte Carlo simulation for 1 μM nucleotide residues at spermine concentrations of (a) 0.7, (b) 1.0, and (c) 1.5 μM. $k_s^+ = 1 \times 10^8$ M^{-1} s^{-1}, $k_s^- = 0.17$ s^{-1}, and $k_m = 200$ s^{-1}.

of times required to attain the limit degree of binding $\theta_\delta = 0.86$. The distribution of times may then be arranged to represent the time dependence of the approach to (and beyond) the limit degree of binding. Since the DNA molecules are converted to the condensed state, when the degree of spermine binding exceeds the limit value, the time dependence obtained by this procedure should represent the condensation reaction. The correspondence should be exact within the context of the model, when the condensation of DNA itself is fast compared to ligand binding. According to the experiments described in the previous section, this condition is fulfilled for the present stopped-flow experiments. By a trial and error procedure, it is possible to evaluate both the association rate constant and the mobility of spermine. The set of reaction curves obtained for an association rate constant $k_s^+ = 1 \times 10^8$ M^{-1} (nucleotides) s^{-1} and a mobility of $k_m = 200$ s^{-1} shown in Figure 7 demonstrates that the experimental curves can be represented with a satisfactory degree of accuracy. Another set of data obtained at a DNA concentration of 2 μM (nucleotides) can also be represented by using the same model parameters.

Simple Model of the Decondensation Reaction. Since the DNA condensation reaction can be described with good accuracy by the threshold model of ligand association, it may be expected that a corresponding model is appropriate for the reverse reaction. Such a model should be valid when the decondensation is controlled by the dissociation of spermine molecules. Evidence for this is obtained by stopped-flow experiments showing a much higher rate of decondensation for spermidine complexes than for spermine complexes. This result indicates that unfolding of the DNA itself is not the rate-determining step in the dissociation of spermine–DNA condensates.

For simplicity, it will be assumed that the dissociation of spermine from DNA may be described by a simple first-order reaction with a rate constant k_s^-. This assumption is justified for stopped-flow dissociation experiments, when the free spermine concentration is maintained at a sufficient low value to preclude reassociation. For a DNA chain with N spermine molecules, dissociation may occur with equal probability at any of the N spermine sites. The probability P of an initially occupied site to be still occupied at time t is given by

$$P = e^{-k_s^- t} \tag{5}$$

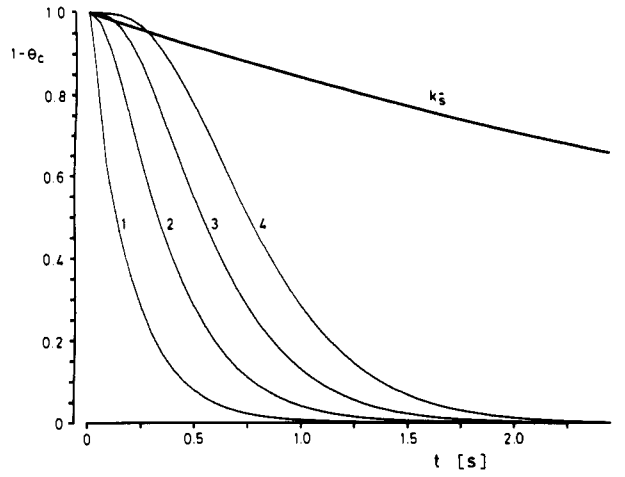

FIGURE 8: Degree of transition $1 - \theta_c$ from condensed to free DNA as a function of time calculated according to eq 4 with $k_s^- = 0.17$ s^{-1}, $N = 30$, and $M = 0$, 1, 2, and 3, corresponding to decondensation after 1, 2, 3, and 4 ligands, respectively, out of 30 are dissociated. The curve denoted by k_s^- shows the degree of ligand binding.

The corresponding probability Q of a site being empty after time t is given by

$$Q = 1 - e^{-k_s^- t} \tag{6}$$

From these probabilities, the distribution of spermine ligands on the DNA lattice may be calculated as a function of time. The probability R of a lattice to lose not more than M ligands up to time t is given by

$$R = \sum_{J=0}^{J=M} \binom{N}{J} P^{N-J} Q^J \tag{7}$$

In close analogy to the condensation reaction (cf. previous section), it may be assumed that the condensed state remains stable as long as the number of dissociated spermine molecules does not exceed a threshold value M. As soon as threshold value is exceeded, the decondensation may proceed rapidly compared to the spermine dissociation. Under these conditions, the probability R as a function of time describes the time course of decondensation.

It is apparent from eq 7 that the rate constant of spermine dissociation cannot be directly determined from a simple decondensation experiment, since the parameters N and M have a strong influence on the decondensation rate. The influence of these parameters is illustrated in Figure 8. When $N = 30$ and $M = 1$, for example, the decondensation rate is much faster than the "elementary" rate of spermine dissociation. The acceleration is simply due to the fact that spermine molecules may dissociate at any of the 30 sites. Obviously, the acceleration effect at a given value of M increases with N. When $M > 1$, the reaction exhibits a period of induction without any decondensation, although spermine molecules dissociate. When the number of dissociated spermine molecules approaches the limit value, the decondensation is observed within a time range that can be very narrow (depending upon the values for N and M). These model calculations may now be compared with the experimental data obtained by stopped-flow measurements. The major part of the DNA is decondensed in about a 1 s, demonstrating an acceleration effect relative to the elementary lifetime of spermine, $1/k_s^- = 5.9$ s, evaluated in the previous section. The experimental curves also show some induction period, indicating the existence of the effect predicted by the model calculations. Due to the approximate nature of the model, it is not attempted to fit precise values of N and M to the experimental data. Obviously, the effective value of N cannot be as high as the total number of spermine

molecules bound to the entire λ-DNA. In this case, the acceleration effect would be much higher than that observed experimentally and/or the decondensation would have a more cooperative appearance with a longer induction period together with a sharp onset of the reaction. The experimental curves can be represented reasonably well with, e.g., $N = 30$ and $M = 2$, suggesting the existence of reaction units comprising approximately 30 spermine molecules, corresponding to about 120 nucleotide residues.

It is also conceivable that DNA decondenses stepwise from the ends of the chain following subsequent steps of spermine dissociation. However, according to the reaction sequence of such a model, it will be difficult to represent the experimentally observed induction period together with the acceleration effect relative to the elementary rate of spermine dissociation.

Field-Jump Experiments. The stopped-flow technique has been very useful to study the DNA condensation by mixing of the components at low concentrations, where the dynamics of the reaction are mainly determined by the rate of ligand binding. However, the time resolution of the stopped-flow technique is not sufficient to study the condensation reaction in the limit of high ligand concentrations, where the dynamics should be mainly determined by the rate of DNA folding. For this purpose, a technique is required with a high time resolution, as, for example, the field-jump technique. Electric field pulses are known to induce dissociation of counterions from polyelectrolytes (Eckstrom & Schmelzer, 1939; Porschke, 1981). Thus, it is expected that an electric field induces dissociation of spermine from condensed DNA followed by decondensation of the DNA. This expectation has been verified by field-jump measurements with condensed DNA using scattered-light detection. The evidence for the field-induced decondensation of DNA is described separately (Porschke et al., 1984).

Field pulses of sufficient amplitude and length, e.g., 25 kV/cm and 150 μs, induce almost complete dissociation of condensed DNA. Thus, field-jump experiments at low reactant concentrations provide results corresponding to those obtained by the stopped-flow technique. The condensation process observed after electric field pulses is accelerated by increasing spermine concentrations. At spermine concentrations around 10 μM, the induction period (cf. previous sections) is already very short and finally disappears at still higher concentrations. For spermine concentrations in the range 300–600 μM, the rate of the condensation process seems to be close to a limit level. Least-squares fits of condensation curves obtained at 600 μM spermine provide three exponentials with time constants of 25 μs, 200 μs, and 2 ms as shown in Figure 9. These numbers should not be regarded as representative of separate molecular processes. It is more likely that the condensation of DNA must be represented by a broad ensemble of time constants. As indicated by measurements at different DNA concentrations and at different times after mixing, the ensemble of condensation time constants is somewhat dependent upon the degree of intermolecular association and the history of the sample [cf. Becker et al. (1979)]. Nevertheless, the distribution of time constants shown in Figure 9 can be regarded as typical for the condensation process at high spermine concentrations. Corresponding measurements at high concentrations of spermidine provide a similar distribution of time constants. The distribution of time constants is also similar for the condensation of λ-DNA and T4 and T7 DNA.

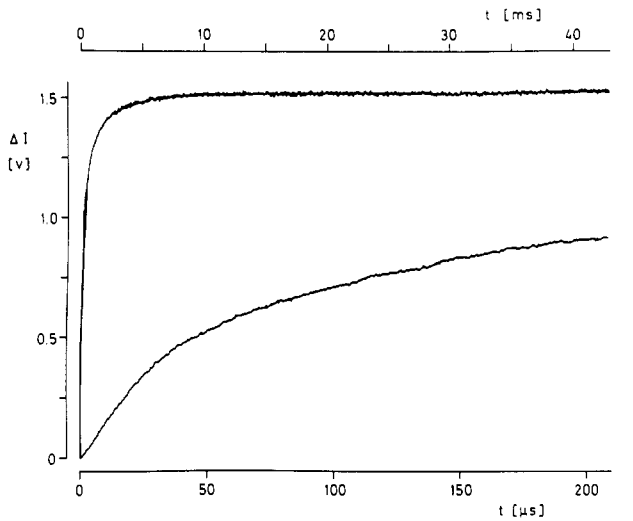

FIGURE 9: Scattered light intensity (arbitrary units) of 5 μM λ-DNA in the presence of 600 μM spermine as a function of time after a field pulse of 21 kV/cm (average value) and 130 μs. Fitting of exponentials provides the time constants 25 μs, 200 μs, and 2 ms with relative amplitudes of 31, 41, and 28%, respectively.

Discussion

Although the spermine-induced condensation of DNA is a relatively simple example for a DNA packing reaction, a quantitative description of this reaction requires already rather complex models. In the present investigation, the description is mainly based on the excluded site model of ligand binding. This model does not describe the special electrostatic effects expected for the interaction of spermine or spermidine molecules with DNA. In previous investigations, the binding of ligands and their influence on the condensation reaction have been described by the polyelectrolyte theory (Manning, 1978; Wilson & Bloomfield, 1979). However, this approach does not consider the influence of excluded-site effects, which is expected to be important as well. The analysis of the transition between the free state and the condensed state performed in the present investigation provides an opportunity to compare the different approaches. The results given in Table I are similar to those obtained previously to a surprisingly large degree. For example, the values for the limit degree of spermine binding, θ_δ, found by Wilson & Bloomfield (1979) are very close to the values given in Table I. The decrease of θ_δ with increasing salt concentration shown in Table I is also similar to previously published values. The binding constants K and their dependence upon the salt concentration I_μ can be described by the equation $\log K = -2.7\ (\pm 0.3)\ \log I_\mu + 1.4\ (\pm 1)$. Previous measurements by equilibrium dialysis (Braunlin et al., 1982) at much higher salt concentrations and lower degrees of binding provided $\log K = -3.3\ (\pm 0.3)\ \log I_\mu + 0.2\ (\pm 0.2)$. When it is considered that these parameters were obtained by different techniques and under completely different conditions, the agreement is surprisingly good. Thus, the equilibrium parameters obtained by the excluded-site model appear to be valid and should not introduce any serious error in the analysis of the kinetic data.

Up to the present investigation, the dynamics of DNA condensation have not been studied in detail. Some observations reported previously seem to be contradictory. Gosule & Schellman (1978) observed a "very rapid" condensation of DNA, which was complete within the few minutes required for their initial measurements, whereas Widom & Baldwin (1983) found that the condensation induced by $Co^{3+}(NH_3)_6$ is slow in the forward direction and fast in the reverse direction. The present measurements demonstrate the existence of two different "condensation" reactions, which are clearly separated on the time scale. It is shown that the *intra*molecular con-

densation is a very fast process in contrast to the very slow reaction of *inter*molecular association. Since it is difficult to measure absolute scattering intensities by fast kinetic techniques, it has not been attempted to characterize the magnitude of light scattering for the different reaction states.

The main emphasis of the present investigation is on the dynamics of the *intra*molecular condensation. The condensation curves observed by scattered-light measurements look unusual, and their explanation seems to be difficult at a first glance. However, a close examination of the molecular mechanism reveals that the type of reaction progress curves found experimentally is consistent with coupling of ligand binding and a "conformation change" of the DNA. Since spermine ligands cover more than a single lattice residue, the ligand binding reaction is described by an excluded-site model. This approach is justified even though the spermine molecules are certainly not rigid. In spite of their flexibility, spermine molecules will "exclude" each other due to electrostatic effects. For example, the binding affinity of a spermine molecule to a gap with three nucleotide residues is expected to be much lower than that to a gap with four residues. Thus, spermine binding to small gaps will be excluded at least at low spermine concentrations around 1 μM. When the spermine concentration is much higher, as, for example, in the field-jump experiment shown in Figure 9, a considerable extent of spermine binding to small gaps is expected. Under these conditions, the rate of DNA condensation will not be affected anymore by excluded-site phenomena and ligand mobility.

When the rate constant of spermine binding to DNA is given in polymer concentration units $k_s^+ = 9 \times 10^{12}$ M^{-1} (polymers) s^{-1}, it appears to be unusually high. However, the effective reaction radius of long DNA molecules is very large. Comparison with corresponding rate constants determined previously (Porschke, 1979) shows that the rate of spermine binding to high molecular weight DNA is in the range expected for a diffusion-controlled reaction. It is also instructive to compare the rate of spermine binding to DNA with the rate on intermolecular condensation (cf. Intermolecular Association under Results). The reactants in the latter case are both of high molecular weight and in a compact conformation. Under these conditions, the rate constant of intermolecular condensation, $k_a^+ = 8.2 \times 10^8$ M^{-1} (polymer) s^{-1}, is likely to be controlled by diffusion, although it is orders of magnitude lower than the rate constant of spermine binding.

Very little information is available on the mobility of ligands along DNA. Thus, it is hardly possible to find a rate constant comparable to the value $k_m = 200$ s^{-1} for spermine movement by one nucleotide residue. It is also difficult to estimate the accuracy of the k_m value due to the approximations inherent in the model and the strong influence of the threshold degree of ligand binding θ_δ. However, the demonstration of significant spermine mobility is not at all unexpected, when compared, for example, with the rather high mobility observed for the complementary strands of double helices along each other, when each of the strands has only one type of base residue (Porschke, 1974). Similar to the mechanism postulated for the sliding of strands in these double helices, the motion of spermine may be accelerated by the intermediate formation of bulged parts of the spermine molecule in its complex with DNA.

More surprisingly than the rate of spermine motion is the high rate of DNA condensation observed in the limit of saturating spermine concentration. It is remarkable how fast the DNA is packed from a disordered wormlike coil to an apparently well-ordered condensed state. It seems that the DNA can be compared with a spring which is kept under tension by electrostatic repulsion; upon release of this tension, the spring collapses almost immediately. The data obtained by scattered-light measurements do not show, however, whether the well-ordered torus is formed already during the primary step of condensation. Torus formation may require rearrangement of DNA strands, which need not be reflected by large changes of the scattered-light intensity.

Obviously, DNA condensation requires bending or kinking. According to studies of the torus structure by electron microscopy, the DNA seems to be bent smoothly rather than kinked (Marx & Ruben, 1983). A process corresponding to smooth bending has been observed recently by measurements of electric dichroism (Diekmann et al., 1982). The time constants associated with bending of relatively short restriction fragments are between 0.1 and 1 μs in the range of chain lengths between 100 and 200 base pairs. A strong increase of the bending time constant with chain length suggests that the condensation time constants observed in the present investigation reflect the spectrum of bending times of the high molecular weight DNA.

The condensation of DNA is a reaction observed with different types of ligands. Although the structure of the condensed DNA can be very different for different ligands, the main feature of the condensation mechanism is expected to be similar in all cases. The binding of ligands to a limit degree of saturation at a reasonable rate will require a relatively high mobility of these ligands in many cases. This will be particularly important for large and rigid ligands as, for example, in the case of histones and the condensation of chromatin.

Acknowledgments

I am greatly indebted to J. Ronnenberg for his expert technical assistance. Most of the equilibrium titrations have been performed by J. Wawrzinek.

Registry No. Spermine, 71-44-3; spermidine, 124-20-9.

References

Becker, M., Misselwitz, R., Damaschun, H., Damaschun, G., & Zirwer, D. (1979) *Nucleic Acids Res. 7*, 1297–1309.

Braunlin, W. H., Strick, T. J., & Record, M. T. (1982) *Biopolymers 21*, 1301–1314.

Chattoray, D. K., Gosule, L. C., & Schellman, J. A. (1978) *J. Mol. Biol. 121*, 327–337.

Diekmann, S., Hillen, W., Morgeneyer, B., Wells, R. D., & Porschke, D. (1982) *Biophys. Chem. 15*, 263–270.

Earnshaw, W. C., & Harrison, S. C. (1977) *Nature (London) 268*, 598–602.

Earnshaw, W. C., King, J., Harrison, S. C., & Eiserling, F. A. (1978) *Cell (Cambridge, Mass.) 14*, 559–568.

Eckstrom, H. C., & Schmelzer, C. (1939) *Chem. Rev. 24*, 367–414.

Epstein, I. R. (1979) *Biopolymers 18*, 2037–2050.

Gosule, L. C., & Schellman, J. A. (1976) *Nature (London) 259*, 333–335.

Gosule, L. C., & Schellman, J. A. (1978) *J. Mol. Biol. 121*, 311–326.

Manning, G. S. (1978) *Q. Rev. Biophys. 11*, 179–246.

Marx, K. A., & Ruben, G. C. (1983) *Nucleic Acids Res. 11*, 1839–1854.

McGhee, J. D., & von Hippel, P. H. (1974) *J. Mol. Biol. 86*, 469–489.

Porschke, D. (1974) *Biophys. Chem. 2*, 83–96.

Porschke, D. (1979) *Biophys. Chem. 10*, 1–16.
Porschke, D. (1981) in *Molecular Electro-Optics* (Krause, S., Ed.) pp 269–284, Plenum Press, New York.
Porschke, D., & Eggers, F. (1972) *Eur. J. Biochem. 26*, 490–498.
Porschke, D., Meier, H. J., & Ronnenberg, J. (1984) *Biophys. Chem.* (in press).
Sperling, L., & Klug, A. (1977) *J. Mol. Biol. 112*, 253–263.
Widom, J., & Baldwin, R. L. (1980) *J. Mol. Biol. 144*, 431–453.
Widom, J., & Baldwin, R. L. (1983) *Biopolymers 22*, 1595–1620.
Wilson, R. W., & Bloomfield, V. A. (1979) *Biochemistry 18*, 2192–2196.

Complete Sequence of the cDNA for Human α_1-Antitrypsin and the Gene for the S Variant†

George L. Long,‡ T. Chandra, Savio L. C. Woo, Earl W. Davie,* and Kotoku Kurachi

ABSTRACT: A 1434 base pair human liver cDNA coding for the entire α_1-antitrypsin protein has been isolated and sequenced. Translation of the coding region into amino acids reveals a precursor molecule which contains a 24 amino acid signal peptide and 394 amino acids present in the mature polypeptide chain. The human gene for the S variant of α_1-antitrypsin has also been subcloned and sequenced. The gene is composed of 10 226 nucleotide bases and is approximately equimolar for all 4 nucleotides. The gene contains four intervening sequences (introns) and 5′ and 3′ noncoding regions which are 54 and 79 nucleotides in length, respectively. A 5.3-kilobase intron exists in the 5′ noncoding region and contains a 143 amino acid open reading frame, an *Alu* family sequence, and a pseudo transcription initiation region. No significant differences in base composition are seen between the introns and those regions corresponding to coding regions of the corresponding mRNA (exons). A sequence of 1951 nucleotides flanking the 5′ end of the gene has also been determined and contains a "TATA" box sequence (TTAAATA) 21 nucleotides upstream from the proposed transcription start site. Comparison of the gene sequence with the cDNA sequence reveals a single base substitution (A → T), which results in a Glu → Val substitution at position 264 in the S variant protein. The position and size of introns, the overall base composition, and the codon preference for the α_1-antitrypsin gene differ from those for the chicken ovalbumin gene even though the two proteins belong to a common protein family, as judged by amino acid sequence homology.

α_1-Antitrypsin (α_1-protease inhibitor) is one of several protease inhibitors found in mammalian blood. It is comprised of a single polypeptide chain (M_r 50000) (Musiani & Tomasi, 1976) containing about 16% carbohydrate attached to three Asn residues (Mega et al., 1980). Approximately 90% of the amino acid sequence has been reported (Carrell et al., 1981). The major physiological role of α_1-antitrypsin is thought to be the inhibition of lysosomal proteases, most notably elastase and collagenase (Kueppers & Black, 1974; Gitlin & Gitlin, 1975; Fagerol, 1976; Sharp, 1976). α_1-Antitrypsin also inhibits several other serine proteases, including trypsin, chymotrypsin, thrombin, kallikrein, and plasmin (Laurell & Jeppsson, 1975).

The normal plasma level of α_1-antitrypsin is about 2 mg/mL. During an acute phase reaction, this level is substantially elevated (Koj, 1974). Individuals with abnormally low levels of circulating α_1-antitrypsin have been shown to be predisposed toward chronic obstructive lung disorders, including emphysema (Kueppers, 1978). Accompanying the lowered circulating levels is an increase in liver tissue levels of α_1-antitrypsin and juvenile cirrhosis (Laurell & Jeppsson, 1975). These facts have led to the proposal that the deficiency of α_1-antitrypsin results from defective cellular processing or transport of the protein in the liver. Over 30 human phenotypes have been identified thus far (Allen et al., 1974; Cox et al., 1980). The most common variant is variant S, which occurs in over 5% of the northern European population (Owen et al., 1976) and as the homozygote (SS) in nearly 2% of populations of Spanish descent (Fagerol, 1976). The only apparent difference between the normal M-type protein and the S protein is a glutamate to valine substitution near the carboxyl end of the protein (Owen et al., 1976). Individuals carrying the S gene exhibit reduced α_1-antitrypsin plama levels (60% for SS, 80% for SM) (Gitlin & Gitlin, 1975), which sometimes result in minor clinical disorders.

Hunt & Dayhoff (1980) were the first to note that α_1-antitrypsin and ovalbumin belong to a common protein family, on the basis of amino acid sequence homology. The nucleic acid structure of the ovalbumin gene and its regulation are known in considerble detail (Benoist et al., 1980; Woo et al., 1981). The cDNA for human and baboon α_1-antitrypsin and the gene for human α_1-antitrypsin have been cloned and partially characterized (Chandra et al., 1981a; Kurachi et al., 1981; Leicht et al., 1982). We now report the entire nucleotide sequence of a normal human liver cDNA clone and the S variant of the α_1-antitrypsin gene. The variant gene was

† From the Department of Biochemistry, University of Washington, Seattle, Washington 98195 (G.L.L., K.K., and E.W.D.), and the Howard Hughes Medical Institute Laboratory, Department of Cell Biology, Baylor College of Medicine, Houston, Texas 77030 (T.C. and S.L.C.W.). *Received February 13, 1984.* This work was supported in part by National Institutes of Health Grants HL 16919 to E.W.D. and HL27509 to S.L.C.W. G.L.L. is the recipient of a Senior Research Fellowship (HL 05962) and K.K. is the recipient of a Research Career Development Award (HL 00404) from the National Institutes of Health. S.L.C.W. is an Investigator of the Howard Hughes Medical Institute.
‡ Present address: Lilly Research Laboratories, Division of Molecular Biology, Eli Lilly and Co., Indianapolis, IN 46285.

0006-2960/84/0423-4828$01.50/0